Surface Waves in Dissipative Poroviscoelastic Layered Half Space: Boundary Element Analyses

F. Dell'Isola, L. A. Igumnov, S. Yu. Litvinchuk, A. A. Ipatov, A. N. Petrov and I. A. Modin

Abstract Wave propagation in a poroelastic layer located on a poroelastic half-space is studied. A fully saturated poroelastic medium is described using Biot's mathematical model with four base functions—pore pressure and skeleton displacements. Viscoelastic behavior of porous medium due to viscoelastic properties of the skeleton is considered. The standard viscoelastic solid model is used. The boundary-value problem of the three-dimensional dynamic poroelasticity is written in terms of Laplace transforms. Direct approach of the boundary integral equation (BIE) method is employed. The boundary-element approach is based on the mixed boundary-element discretization of surface with generalized quadrangular elements. Time-step scheme for numerical inversion of the Laplace transforms is used obtain the solution of boundary value problem. To verify the boundary-element model, poroelastic solutions are compared with elastic ones.

Keywords Boundary element method · Biot's model · Poroviscoelasticity · Half space

1 Introduction

Currently, mathematical modeling is one of the main tools to analyze and optimize oil and gas fields development, to solve the problems of seismic construction and bioengineering [1–7]. The model of poroelastic medium, allowing to describe fluid filtration in pores in together with a full-scale mechanical model of the stress-strain state of medium is usually used to describe the "solid"–"fluid" system.

Modern forms of these models were introduced by Biot [8]. Biot's model correctly describes processes of elastic porous medium deformation and fluid flow in that medium. It is assumed that the space containing poroelastic medium is filled with a

F. Dell'Isola · L. A. Igumnov (✉) · S. Yu. Litvinchuk · A. A. Ipatov · A. N. Petrov · I. A. Modin
Research Institute for Mechanics, National Research Lobachevsky State University of Nizhni Novgorod, Nizhni Novgorod, Russia
e-mail: igumnov@mech.unn.ru

H. Altenbach et al. (eds.), *Dynamical Processes in Generalized Continua and Structures*, Advanced Structured Materials 103,
https://doi.org/10.1007/978-3-030-11665-1_17

two-phase material, and one phase corresponds to the elastic skeleton, and the another one to the fluid in pores. Both phases are present at each point of the physical space, and the phase distribution in space is described by macroscopic quantities such as porosity.

Biot's model allows us to solve a number of particular problems, among which the problems of wave propagation in homogeneous and layered poroelastic half-spaces are of particular interest [9–17]. However, the increasing complexity of computational schemes for boundary value problems requires the involvement of advanced methods such as boundary elements method (BEM). Possessing high accuracy and rigor of the approach, BEM is the most suitable method for considering nonstationary processes in semi-infinite bodies, since it ensures automatic fulfillment of the conditions for solution behavior at infinity. Despite the noted advantages of BEM, the possibility of modeling the poroelastic dynamics is mainly determined by the presence of the corresponding boundary integral equations (BIE) and fundamental solutions. Fundamental solutions and BIE of the dynamic theory of poroelasticity were obtained in [18–21]; in [22–25] different variants of boundary element schemes for the solution of problems in porodynamics are presented and results of numerical experiments are provided. Results of boundary element modeling of dynamics of poroelastic halfspaces are presented in [26–30].

The principal difference of poroelastic formulation from elastic and viscoelastic is that it allows to take into account the influence exerted by the fluid moving in pores on the behavior of the medium as a whole. Historically, on the basis of Biot's theory, the existence of two longitudinal waves—fast and slow in porous medium was predicted. The slow longitudinal wave is caused by the movement of fluid particles of the pores relative to the porous skeleton and is peculiar only to porous media. In addition, the frictional interaction of viscous fluid and a skeleton leads to a significant dissipation of energy in the medium, which demonstrates viscoelastic behavior [31, 32]. The viscoelastic behavior of poroelastic medium can also be due to the viscoelastic properties of the skeleton [33–35]. Some results of simulation of wave processes in poroelastic solids with the use of BIE, BEM and various models of viscoelastic behavior of the skeleton are presented in [36–38].

The paper presents the modeling of wave propagation in homogeneous and inhomogeneous poroviscoelastic in semi-infinite bodies using time-step BEM scheme. A poroviscoelastic layer on a semi-elastic halfspace is considered as an implementation of the inhomogeneity model.

2 Problem Formulation

Basic poroelastic material is a two-phase material consisting of an elastic skeleton and compressible fluid or gas filler. Porous material of a volume V can be constructed as follows:

$$V = V^f + V^s \tag{1}$$

where V is the total volume, V^f is the summary pore volume and V^s is the volume of the skeleton. It is assumed that filler can openly seep through the pores and all closed pores are assumed as a part of the skeleton. Then a correspondence principle is applied to the skeleton, so we extend poroelastic formulation to poroviscoelasticity.

Considering a boundary-value problem for Biot's model of fully saturated poroelastic continuum in Laplace domain in terms of four unknowns (displacements $\bar{u}_i$ and pore pressure $\bar{p}$) the set of differential equations take the following form [30]:

$$\begin{aligned} &G\bar{u}_{i,jj} + \left(K + \frac{G}{3}\right)\bar{u}_{j,ij} - (\psi - \beta)\bar{p}_{,i} - s^2(\rho - \beta\rho_f)\bar{u}_i = -\bar{F}_i, \\ &\frac{\beta}{s\rho_f}\bar{p}_{,ii} - \frac{\phi^2 s}{R}\bar{p} - (\psi - \beta)s\bar{u}_{i,i} = -\bar{a}, \quad x \in \Omega, \end{aligned} \tag{2}$$

Boundary conditions:

$$\begin{aligned} &\bar{u}(x,s) = f(x,s), \quad x \in \Gamma^u, \quad \bar{u} = (\bar{u}_1, \bar{u}_2, \bar{u}_3, \bar{p}), \\ &\bar{t}(x,s) = g(x,s), \quad x \in \Gamma^\sigma, \quad \bar{t} = \left(\bar{t}_1, \bar{t}_2, \bar{t}_3, \bar{q}\right), \end{aligned}$$

where Γ^u and Γ^σ denotes boundaries for boundary conditions of 1st and 2nd kind respectively, G, K are elastic moduli, $\phi = V^f/V$ is porosity, $\bar{F}_i$, $\bar{a}$ are bulk body forces.

$$\beta = \frac{\kappa\rho_f\phi^2 s}{\phi^2 + s\kappa(\rho_a + \phi\rho_f)}, \psi = 1 - \frac{K}{K_s} \text{and } R = \frac{\phi^2 K_f K_s^2}{K_f(K_s - K) + \phi K_s(K_s - K_f)}$$

are constants reflecting interaction between skeleton and filler, κ is permeability. Further, $\rho = \rho_s(1-\phi) + \phi\rho_f$ is a bulk density, ρ_s, ρ_a, ρ_f are solid, apparent mass density and filler density respectively, K_s, K_f are elastic bulk moduli of the skeleton and filler respectively. Apparent mass density $\rho_a = C\phi\rho_f$ was introduced by Biot to describe dynamic interaction between fluid and skeleton. C is a factor depending on the pores geometry and excitation frequency.

The governing equation system (2) in matrix form can be written as follows:

$$B\bar{u} = F, \quad \bar{u}^{\mathrm{T}} = (\bar{u}_i, p), i = 1, 3$$

$$\mathrm{B} = \begin{bmatrix} G\nabla^2 + \left(K + \frac{1}{3}G\right)\partial_i\partial_j - s^2(\rho - \beta\rho_f) & -(\psi - \beta)\partial_i \\ -s(\psi - \beta)\partial_j & \frac{\beta}{s\rho_f}\nabla^2 - \frac{\phi^2 s}{R} \end{bmatrix}.$$

Boundary conditions are:

$$u(x,s) = f(x,s) \text{ on } \Gamma^u, t_n(x,s) = g(x,s) \text{ on } \Gamma^\sigma.$$

In present paper we consider piecewise homogeneous solid Ω in Euclidian space R^3 with coordinate system $Ox_1x_2x_3$. Solid Ω is enclosed with boundary denotes as Γ, boundaries of Ω_k $(k = 1, \ldots, K)$ are denoted as Γ_k. Each part Ω_k is assumed to be isotropic. Material parameters of each Ω_k are denotes by upper index « k » So, governing equations for each part Ω_k in matrix form take a following form:

$$B^k \bar{u}^k = 0, \quad \bar{u}^k = (\bar{u}_i^k, p^k),\ i = 1, 3$$

$$\begin{bmatrix} G^k\nabla^2 + \left(K^k + \frac{1}{3}G^k\right)\partial_i\partial_j - s^2(\rho^k - \beta^k\rho_f^k) & -(\psi^k - \beta^k)\partial_i \\ -s(\psi^k - \beta^k)\partial_j & \frac{\beta^k}{s\rho_f^k}\nabla^2 - \frac{\phi^{k2}s}{R^2} \end{bmatrix}$$

where $\bar{u}^k(x, s)$—generalized displacements vector at point $x = (x_1, x_2, x_3)$. Assumed that $u^k(x, t)$ fulfill zero initial condition:

$$u^k(x,\ 0) = u^k(x,\ 0) = 0$$

Following boundary conditions are employed for each Ω_k:

$$u_l^k(x, t) = f_l^k(x, t),\ x \in \Gamma^u \cap \Gamma_k, \quad l = \overline{1, 3};$$
$$t_l^k(x, t) = g_l^k(x, t), \quad x \in \Gamma^\sigma \cap \Gamma_k;$$
$$u_l^k(x, t) = u_l^m(x, t),\ t_l^k(x, t) = -t_l^m(x, t),\ x \in \Gamma'_{km}\,.$$

Here, Γ^u and Γ^σ are parts of boundary Γ of body Ω, along which displacements and surface tractions, respectively, are assigned; Γ'_{ks} is the contact boundary of parts Ω_k and Ω_s. Functions $f_l^k(x, t)$ and $g_l^k(x, t)$ are assigned functions of the coordinates and time.

Poroviscoelastic solution is obtained from poroelastic solution by means of the elastic-viscoelastic correspondence principle, applied to skeleton's moduli K and G in Laplace domain. Forms of functions $\bar{K}(s)$ and $\bar{G}(s)$ depend on chosen viscoelastic model.

In present paper, standard linear solid model is employed:

$$\bar{K}(s) = K^\infty \cdot \left[(\chi - 1)\frac{s}{s + \eta} + 1\right],$$
$$\bar{G}(s) = G^\infty \cdot \left[(\chi - 1)\frac{s}{s + \eta} + 1\right]$$

The equilibrium and instantaneous values of the relaxation function associated with material modules are connected as follows:

$$\chi = K^0/K^\infty = G^0/G^\infty$$

Equilibrium and instantaneous values are denoted by «∞» and «0» respectively.

3 Boundary-Element Approach

Boundary-value problem can be reduced to the BIE system as follows [26–30]:

$$\frac{1-\alpha_\Omega}{2}\upsilon_i(\mathbf{x},s)+\int\limits_\Gamma\Big(T_{ij}(\mathbf{x},\mathbf{y},s)\upsilon_i(\mathbf{y},s)-T^0_{ik}(\mathbf{x},\mathbf{y},s)\upsilon_i(\mathbf{x},s)-U_{ij}(\mathbf{x},\mathbf{y},s)t_i(\mathbf{y},s)\Big)d\Gamma=0,$$

where $\mathbf{x},\mathbf{y}\in\Gamma$ U_{ij}, T_{ij} are fundamental and singular solutions, T^0_{ij} contains the isolated singularities, $\mathbf{x}\in\Gamma$ is an arbitrary point. Coefficient α_Ω equals to 1 in case of finite domain and -1 in case of infinite domain.

Boundary surface of our homogeneous solid is discretized by quadrangular and triangular elements and triangular elements are assumed as singular quadrangular elements. The Cartesian coordinates of an arbitrary point of the element are expressed through the coordinates of the nodal points of this element, using shape functions of the local coordinates. Shape functions are quadratic polynomials of interpolation. We use reference elements: square $\xi=(\xi_1,\xi_2)\in[-1,\ 1]^2$ and triangle $0\le\xi_1+\xi_2\le 1$, $\xi_1\ge 0,\xi_2\ge 0$, and each boundary element is mapped to a reference one by the following formula:

$$y_i(\xi)=\sum_{l=1}^{8}N^l(\xi)y_i^{\beta(k,l)},\qquad i=1,\ 2,\ 3,$$

where l is local node number in element k, $\beta(k,l)$ is global node number, $N^l(\xi)$ are shape functions. Goldshteyn's displacement-stress mixed model is performed. To discretize the boundary surface eight-node biquadratic quadrilateral elements are used, generalized displacements and tractions are approximated by linear and constant shape functions, respectively.

Subsequent application of collocation method leads to the system of linear equations. As with the collocation nodes we take the approximation nodes of boundary functions. Gaussian quadrature are used to calculate integrals on regular elements. However, if an element contains a singularity, algorithm of singularity avoiding or order reducing is applied. When singularity is excluded we use an adaptive integration algorithm. An appropriate order of Gaussian quadrature is chosen from primarily known necessary precision, if it is impossible, the element is subdivided to smaller elements recursively.

Solving the system of linear equations leads to the solution of the initial boundary-value problem in Laplace domain.

4 Laplace Transform Inversion

Consider a method based on the theorem of the integration of the original—the stepped method of numerical inversion of Laplace transform. Consider the following integral:

$$y(t) = \int_0^t f(\tau)d\tau. \tag{3}$$

Integral (3) gives rise to Cauchy problem for an ordinary differential equation:

$$\frac{d}{dt}x(t) = sx(t) + C, x(0) = 0.$$

Integral (3) is substituted for by a quadrature sum, weighting factors of which are determined using Laplace representation $\overline{f}$ and the linear multi-step method [39]. Further derivation is based on the results of those works. The traditional stepped method of integrating the original consists in that integral (3) is calculated using the following relation:

$$y(0) = 0, \quad y(n\Delta t) = \sum_{k=1}^{n} \omega_k(\Delta t), \quad n = 1, \ldots N,$$
$$\omega_n(\Delta t) = \frac{R^{-n}}{2\pi} \int_0^{2\pi} \bar{f}\left(\frac{\gamma\left(Re^{i\varphi}\right)}{\Delta t}\right) e^{-in\varphi} d\varphi$$

where Δt is time step; $\gamma(z) = 3\big/2 - 2z + z^2\big/2.$; n is number of a time step, $n = 0, N$; R is parameter of the method.

The traditional method uses a constant-step trapezoid method for integrating. Consider the following formula of constructing ω_n based on a variable step:

$$\omega_n(\Delta t) = \frac{R^{-n}}{2\pi} \sum_{k=0}^{L-1} \left[\bar{f}\left(\frac{\gamma(Re^{in\varphi_k})}{\Delta t}\right) e^{-in\varphi_k} + \bar{f}\left(\frac{\gamma(Re^{in\varphi_{k+1}})}{\Delta t}\right) e^{-in\varphi_k+1} \right] \frac{(\varphi_{k+1} - \varphi_k)}{2}.$$

5 Numerical Example

The problem of the Heaviside-type load $H(t)$ acting on the surface of a poroelastic layer located on a poroelastic halfspace is considered (Fig. 1). Two variants of geometry problem are considered—with a layer thickness of 5 and 10 m. A vertical load $t_3 = -1000$ N/m$^2 \cdot H(t)$ is specified on a surface area of 1 m^2, the rest of the surface is traction-free and permeable. At the boundary between the layer and halfspace, the flow, the force, displacements and pore pressure are assumed to be unknown

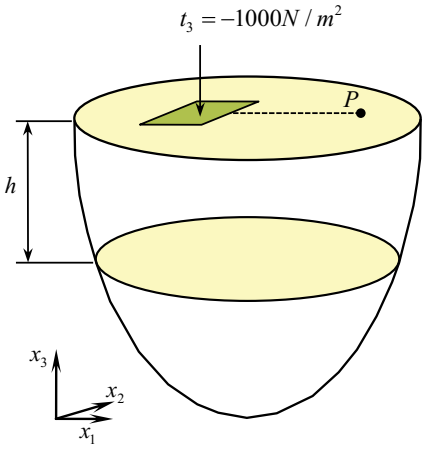

Fig. 1 Layered half space under vertical load

functions. The parameters of the poroelastic soil and the rock are given in Table 1. Moduli characterizing the elastic behavior of the porous material in accordance with the drained and undrained models are also given in Table 1. Dynamic responses of vertical displacements u_3 at the point P, located at a distance of 10 m from the area of load application are shown in Figs. 2, 3, 4, 5, 6, 7, 8, 9 and 10.

Table 1 Poroelastic constants for various materials

Parameter	Poroelastic		Elastic drained		Elastic undrained	
	Rock	Soil	Rock	Soil	Rock	Soil
Bulk modulus K [N/m^2]	$8 \cdot 10^9$	$2.1 \cdot 10^8$	$8 \cdot 10^9$	$2.1 \cdot 10^8$	$1.57 \cdot 10^{10}$	$4.83 \cdot 10^9$
Shear modulus G [N/m^2]	$6 \cdot 10^9$	$9.8 \cdot 10^9$	$6 \cdot 10^9$	$9.8 \cdot 10^9$	$6 \cdot 10^9$	$9.8 \cdot 10^9$
Density ρ [kg/m^3]	2458	1884	2458	1884	2458	1884
Solid bulk modulus K_s [N/m^2]	$3.6 \cdot 10^{10}$	$1.1 \cdot 10^{10}$	–		–	
Fluid bulk modulus K_f [N/m^2]	$3.3 \cdot 10^9$	$3.3 \cdot 10^9$	–		–	
Fluid density ρ_f [kg/m^3]	1000	1000	–		–	
Porosity φ[−]	0.19	0.48	–		–	
Permeability κ [m^4/(N · s)]	$1.9 \cdot 10^{-10}$	$3.55 \cdot 10^{-9}$	–		–	

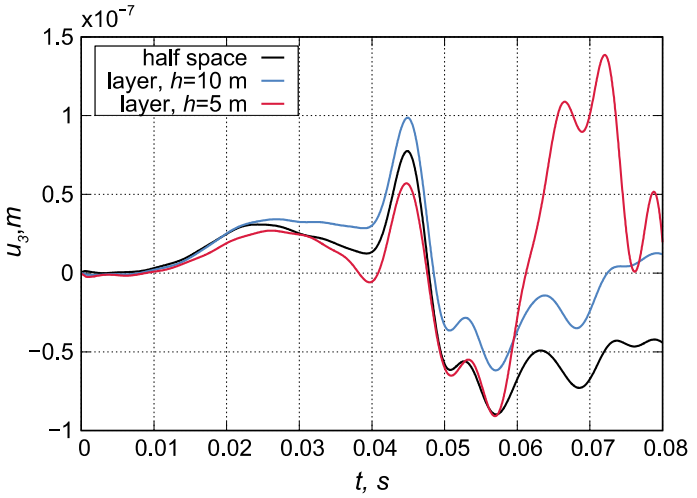

Fig. 2 Displacement at point P versus time: different depth of the layer

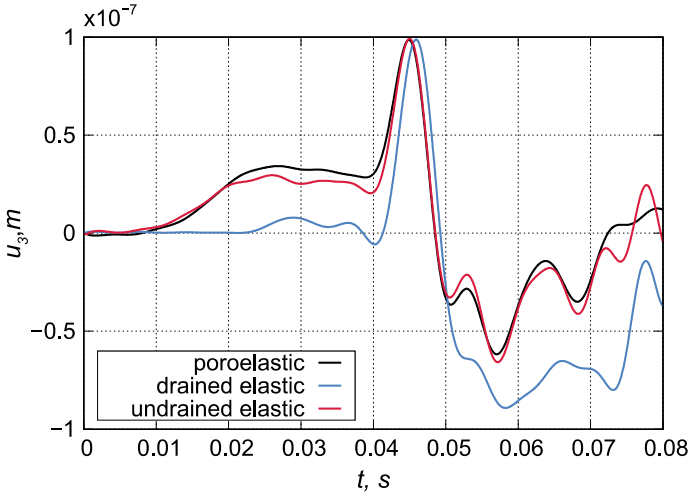

Fig. 3 Vertical displacement at point P versus time. Comparison of poroelastic and elastic solutions of the soil and rock for layer of 5 m depth

Figure 2 presents the comparison of vertical displacements, calculated for the layer with thicknesses of 5 m и 10 m and labeled $u_3^{5\text{ m}}$ and $u_3^{10\text{ m}}$, respectively. Figure 2 also represents solutions for displacements $\left(u_3^{hs}\right)$, calculated for the same values of the halfspace material parameters, which describe layer material. It can be seen that until the appearance of the fast longitudinal wave ($t \approx 0.01$ s) all three curves are almost graphically indistinguishable, however, quantitative differences are observed further. In the moment of Rayleigh wave ($t \approx 0.047$ s) appearance and up to the moment $t \approx$

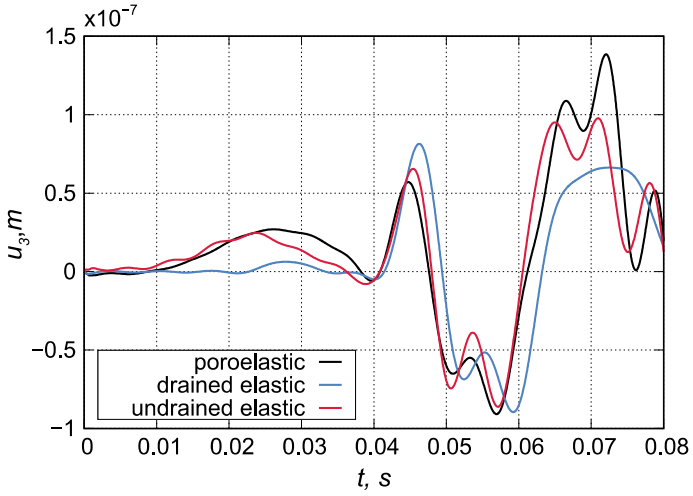

Fig. 4 Vertical displacement at point *P* versus time. Comparison poroelastic and elastic solutions of the soil and rock for layer of 10 m depth

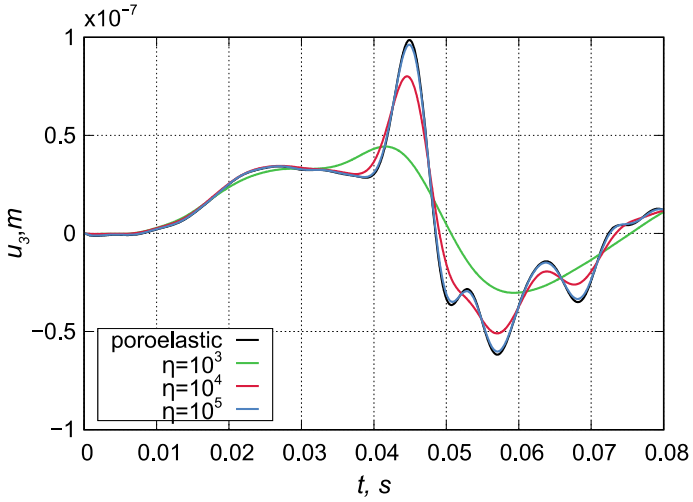

Fig. 5 Vertical displacement at point *P* versus time. Poroviscoelastic dynamic analysis of the soil and rock for layer of 10 m depth

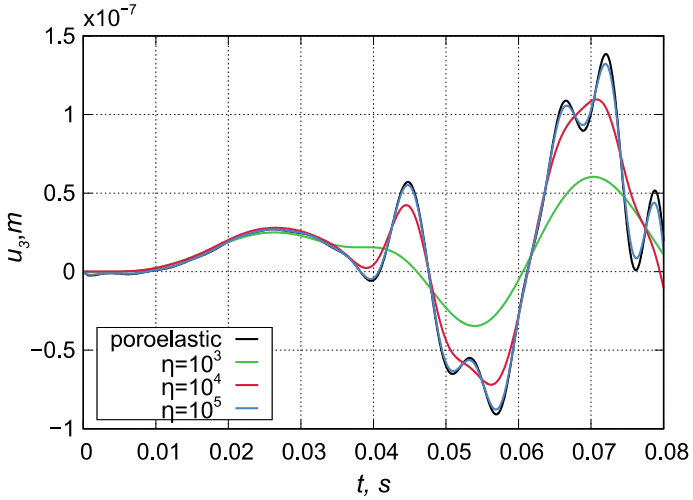

Fig. 6 Vertical displacement at point *P* versus time. Poroviscoelastic dynamic analysis of the soil and rock for layer of 5 m depth

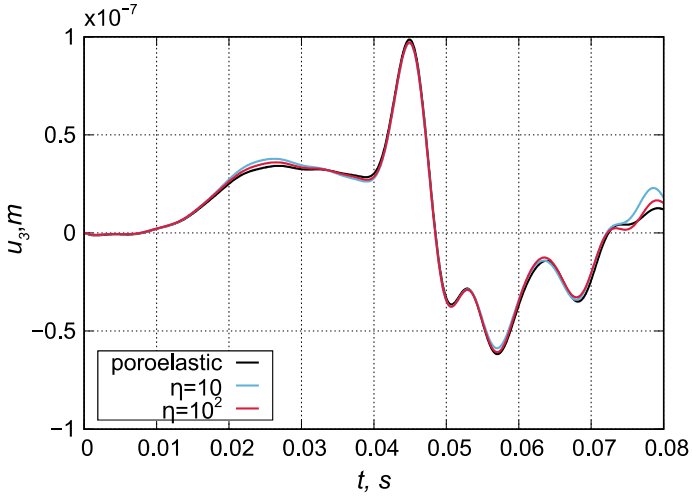

Fig. 7 Vertical displacement at point *P* versus time. Poroviscoelastic dynamic analysis of the rock for layer of 10 m depth

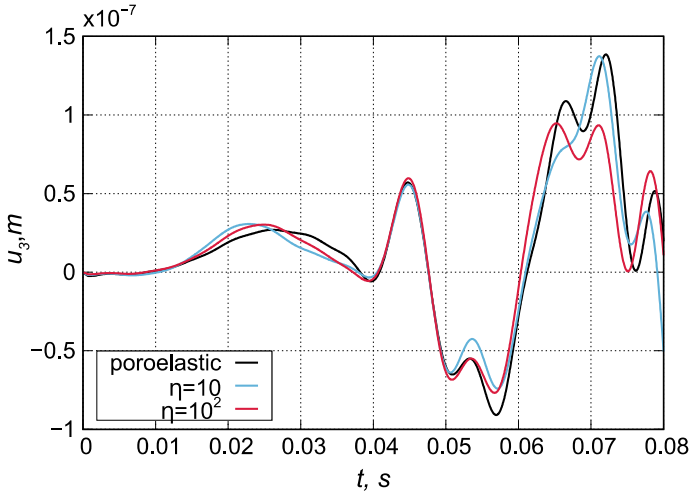

Fig. 8 Vertical displacement at point *P* versus time. Poroviscoelastic dynamic analysis of the rock for layer of 5 m depth

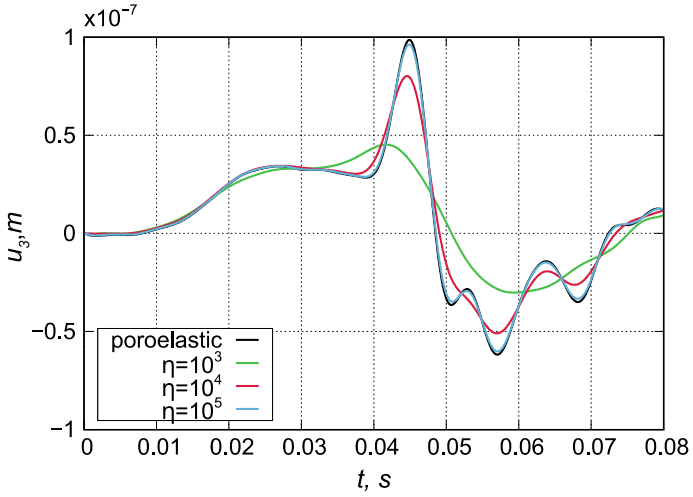

Fig. 9 Vertical displacement at point *P* versus time. Poroviscoelastic dynamic analysis of the soil for layer of 10 m depth

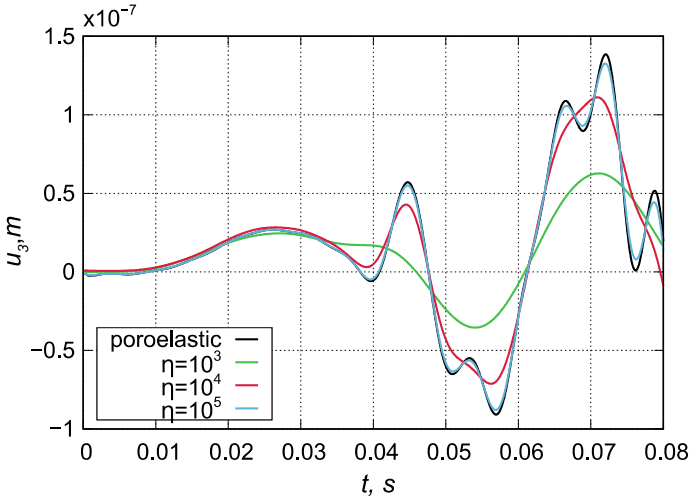

Fig. 10 Vertical displacement at point P versus time. Poroviscoelastic dynamic analysis of the soil for layer of 5 m depth

0.057 s the displacement behavior is described by the relation $u_3^{5\,\mathrm{m}} \leq u_3^{hs} \leq u_3^{10\,\mathrm{m}}$. The time moment $t \approx 0.057$ s is marked by an increase in displacements $u_3^{5\,\mathrm{m}}$ and $u_3^{10\,\mathrm{m}}$, and the displacements $u_3^{5\,\mathrm{m}}$ increase much more rapidly and exceed $u_3^{10\,\mathrm{m}}$ and u_3^{hs} by amplitude. The observed effect is explained by the influence of longitudinal waves reflected from the halfspace and is less noticeable in the case of a larger layer thickness due to the considerable wave dispersion in porous medium.

Figures 3 and 4 show the comparison of displacements $u_3^{5\,\mathrm{m}}$ and $u_3^{10\,\mathrm{m}}$ ith the displacements calculated using elastic models, respectively. In both cases, the solution obtained from the undrained material model is the best approximation to the poroelastic solution, but the differences are also observed here due to the influence of the waves reflected from the halfspace. Figure 4 shows that the amplitude of the Rayleigh wave of the poroelastic solution is smaller than the corresponding amplitudes of the elastic solutions.

In order to obtain poroviscoelastic solutions standard linear solid model is employed. Parameter η characterize viscosity, and parameter $\chi = K^0/K^\infty = G^0/G^\infty$ characterize dependence between equilibrium and instantaneous values of material modules. In further computations parameter $\chi = 4$.

Figures 5, 6, 7, 8, 9 and 10 demonstrate the influence of viscoelastic properties of the skeleton on the dynamic response of vertical displacements. Figures 5 and 6 represent the vertical displacements on the surface of a viscoelastic layer located on a poroelastic halfspace. With increase of the parameter η, it is seen that viscoelastic solution approaches poroelastic solution, but decrease of η leads to reduce of displacement amplitude. The influence of dissipative effects on the surface displacements of the five-meter layer is especially noticeably at $\eta = 10^3$ when the amplitude

of the Rayleigh wave displacement does not exceed the amplitude of the longitudinal wave displacements (Fig. 6).

Figures 7 and 8 represent vertical displacements on the surface of poroelastic layer located on a porous viscoelastic halfspace. It can be observed that the dissipative effects associated with viscoelastic behavior of the halfspace have minor effect on the dynamic responses of displacements on the surface of both the 5 and 10 m layers.

Figures 9 and 10 show vertical displacements on the surface of a viscoelastic layer located on the poroelastic halfspace. In this case, the displacement curves almost coincide with the displacement curves presented in Figs. 5 and 6, and the corresponding comments can be repeated. Taking into account the comments made regarding the results in Figs. 7 and 8, we can say that the dynamic responses of the surface displacements of the layer are mainly affected by the viscoelastic properties of the layer.

6 Conclusion

The Biot's mathematical model of poroelastic material is given in the present paper. The systems of equations of the theory of dynamic poroelasticity and the formulation of boundary value problems in Laplace transforms are formulated. The technique of numerical inversion of the Laplace transform based on step method is presented. The boundary-element solutions for a problem involving a vertical load acting on the surface of a poroelastic layer located on a poroelastic halfspace are presented. The effect of the viscoelastic properties of the skeleton of porous material on vertical displacements on the surface layer is studied. It is noted, that the form of wave patterns is mainly influenced by dissipative effects caused by the viscoelastic behavior of the layer.

Acknowledgements This work was supported by a grant from the Government of the Russian Federation (contract No. 14.Y26.31.0031).

References

1. Chapelle, D., Gerbeau, J.-F., Sainte-Marie, J., Vignon-Clementel, I.E.: A poroelastic model valid in large strains with applications to perfusion in cardiac modeling. Comput. Mech. **46**, 91–101 (2010). https://doi.org/10.1007/s00466-009-0452-x
2. Phillips, P.J., Wheeler, M.F.: A coupling of mixed and continuous Galerkin finite element methods for poroelasticity. I. The continuous in time case. Comput. Geosci. **11**, 131–144 (2007). https://doi.org/10.1007/s10596-007-9045-y
3. Phillips, P.J., Wheeler, M.F.: A coupling of mixed and continuous Galerkin finite element methods for poroelasticity. II. The discrete-in-time case. Comput. Geosci. **11**, 145–158 (2007). https://doi.org/10.1007/s10596-007-9044-z

4. Phillips, P.J., Wheeler, M.F.: A coupling of mixed and discontinuous Galerkin finite element methods for poroelasticity. Comput. Geosci. **12**, 417–435 (2008). https://doi.org/10.1007/s10596-008-9082-1
5. Causin, P., Guidoboni, G., Harris, A., Prada, D., Sacco, R., Terragni, S.: A poroelastic model for the perfusion of the lamina cribrosa in the optic nerve head. Math. Biosci. **257**, 33–41 (2014). https://doi.org/10.1016/j.mbs.2014.08.002
6. Sobhaniaragh, B., Mansur, W.J., Peters, F.C.: Three-dimensional investigation of multiple stage hydraulic fracturing in unconventional reservoirs. J. Petrol. Sci. Eng. **146**, 1063–1078 (2016)
7. Nazarova, L.A., Nazarov, L.A.: Evolution of stresses and permeability of fractured-and-porous rock mass around a production well. J. Min. Sci. **52**(3), 424–431 (2016)
8. Biot, M.A.: General theory of three dimensional consolidation. J. Appl. Phys. **12**, 155–164 (1941). https://doi.org/10.1063/1.1712886
9. Jin, B., Liu, H.: Horizontal vibrations of a disk on a poroelastic half-space. Soil Dyn. Earthq. Eng. J. **19**(4), 269–275 (2000)
10. Jin, B., Liu, H.: Rocking vibrations of rigid disk on saturated poroelastic medium. Soil Dyn. Earthq. Eng. J. **19**(7), 469–472 (2000)
11. Jin, B., Liu, H.: Vertical dynamic response of a disk on a saturated poroelastic halfspace. Soil Dyn. Earthq. Eng. J. **18**(6), 437–443 (1999)
12. Gazetas, G., Petrakis, E.: Offshore caissons on porous saturated soil. In: Parkash, S. (ed.), Proceedings of International Conference on Recent Advances in Geotechnical Earthquake Engineering and Soil Dynamics, pp. 381–386. University of Missouri-Rolla, Rolla (1981)
13. Degrande, G., De Roeck, G., Van Den Broeck, P.: Wave propagation in layered dry, saturated and unsaturated poroelastic media. Int. J. Solids Struct. **35**(34–35), 4753–4778 (1998)
14. Paul, S.: On the displacements produced in a porous elastic half-space by an impulsive line load (non-dissipative case). Pure Appl. Geophys. **114**(4), 605–614 (1976)
15. Paul, S.: On the disturbance produced in a semi-infinite poroelastic medium by a surface load. Pure Appl. Geophys. **114**(4), 615–627 (1976)
16. Philippacopoulos, A.J.: Axisymmetric vibrations of disk resting on saturated layered half-space. J. Eng. Mech. **115**(10), 2301–2322 (1989)
17. Philippacopoulos, A.J.: Buried point source in a poroelastic half-space. J. Eng. Mech. **123**(8), 860–869 (1997)
18. Schanz, M.: Poroelastodynamics: linear models, analytical solutions, and numerical methods. Appl. Mech. Rev. **62**, 030803 (2009). https://doi.org/10.1115/1.3090831
19. Gatmiri, B., Kamalian, M.: On the fundamental solution of dynamic poroelastic boundary integral equations in time domain. Int. J. Geomech. **2**(4), 381–398 (2002)
20. Gatmiri, B., Nguyen, K.V.: Time 2D fundamental solution for saturated porous media with incompressible fluid. Commun. Numer. Methods Eng. **21**(3), 119–132 (2005)
21. Seyerafian, S., Gatmiri B., Nourzad, A.: Green functions for a continuously nonhomogeneous saturated media. Int. J. Comput. Methods Eng. Sci. (CMES) **15(2),** 115–125 (2006)
22. Gatmiri, B., Eslami, H.: Scattering of harmonic waves by a circular cavity in a porous medium: complex functions theory approach. Int. J. Geomech. **7**(5), 371–381 (2007)
23. Theodorakopoulos, D.D., Beskosa, D.E.: Application of Biot's poroelasticity to some soil dynamics problems in civil engineering. Soil Dyn. Earthq. Eng. **26**, 666–679 (2006)
24. Dominguez, J.: Boundary elements in dynamics. Computational Mechanics Publications, Southampton (1993)
25. Albers, B., Savidis, S., Tasan, H.E., Von Estroff, O., Gehlken, M.: BEM and FEM results of displacements in a poroelastic column. Int. J. Appl. Math. Comput. Sci. **22**(4), 883–896 (2012)
26. Igumnov, L.A., Petrov, A.N., Vorobtsov, I.V.: Analysis of 3D poroelastodynamics using BEM based on modified time-step scheme. IOP Conf. Ser.: Earth Environ. Sci. **87**(8), 082022 (2017)
27. Igumnov, L., Ipatov, A., Belov, A., Petrov, A.: A combined application of boundary-element and Runge-Kutta methods in three-dimensional elasticity and poroelasticity. EPJ Web Conf. **94**, 04026 (2015)
28. Igumnov, L.A., Litvinchuk, S.Y., Petrov, A.N., Belov, A.A.: Boundary-element modeling of 3-D poroelastic half-space dynamics. Adv. Mater. Res. **1040**, 881–885 (2014)

29. Dineva, P., Datcheva, M., Schanz, T.: BIEM for seismic wave propagation in fluid saturated multilayered media. In: Proceedings of the 6th European Conference on Numerical Methods in Geotechnical Engineering—Numerical Methods in Geotechnical Engineering. (2006)
30. Schanz, M., Antes, H.: Waves in poroelastic half space: boundary element analyses. In: Ehlers, W., Bluhm, J. (eds.) Porous Media. Springer, Berlin, Heidelberg (2002)
31. Mow, V.C., Lai, W.M.: Recent developments in synovial joint biomechanics. SIAM Rev. **22**, 275 (1980)
32. Mow, V.C., Roth, V., Armstrong, C.G.: Biomechanics of joint cartilage. In: Frankel, V.H., Nordin, M.A. (eds.) Basic biomechanics of the skeletal system, p. 61. Lea and Febiger, Philadelphia (1980)
33. Ehlers, W., Markert, B.: On the viscoelastic behaviour of fluid-saturated porous materials. Granul. Matter. **2**(3), 153–161 (2000)
34. Mak, A.F.: The apparent viscoelastic behaviour of articular cartilage—the contribution from the intrinsic matrix viscoelasticity and interstitial fluid flows. J. Biomech. Eng. **108**, 123–130 (1986)
35. Banks, H.T., Bekele-Maxwell, K., Bociu, L., Noorman, M., Guidoboni, G.: Sensitivity analysis in poro-elastic and poro-visco-elastic models with respect to boundary data. Q. Appl. Math. **75**(4), 697–735 (2017)
36. Ipatov, A.A., Igumnov, L.A., Belov, A.A.: Boundary element method in three dimensional transient poroviscoelastic problems. Springer Proc. Phys. **193**, 331–346 (2017)
37. Igumnov, L.A., Litvinchuk, SYu., Belov, A.A., Ipatov, A.A.: Boundary element formulation for numerical surface wave modelling in poroviscoelastisity. Key Eng. Mater. **685**, 172–176 (2016)
38. Wuttke, F., Dineva, P., Fontara, I.-K.: Influence of poroelasticity on the 3D seismic response of complex geological media. J. Theor. Appl. Mech. **47**(2), 34–60 (2017)
39. Igumnov, L.A., Petrov, A.N.: Dynamics of partially saturated poroelastic solids by boundary-element method. PNRPU Mech. Bull. **47**(3), 47–61 (2016)